SLS-TME-TA-2000-0152
June 2000

Algorithms for dynamic alignment of the SLS storage ring girders

Andreas Streun

Paul Scherrer Institut
CH-5232 Villigen PSI
Switzerland

Algorithms for dynamic alignment of the SLS storage ring girders

Andreas Streun, PSI

June 26, 2000

1 Introduction

The innovative dynamic alignment system of the SLS storage ring [1] is based on a 5-point mover system for each of the 48 magnet girders [2]. The girder positions are surveyed initially and periodically by means of reference marks attached to the girder itself and to the magnets mounted rigidly to the girder. During operation the girder position is controlled by the hydrostatic levelling system (HLS) for vertical and roll motions, and by the horizontal positioning system (HPS) for horizontal motions. Finally a beam based girder alignment may be performed by using the girder mover system like corrector magnets for closed orbit correction.

In this report we give the algorithms required to get the girder positions from survey, HLS and HPS, and to set the girder positions by means of the mover system. We will also show simulation results for the beam based girder alignment procedure.

Large figures and tables have been moved to the end of the note. Test programs implementing the algorithms are available at [8].

2 Girder motion

The girder coordinate system as shown in figures 4 is a right hand system with

- x pointing outside, away from the machine center
- y pointing up,
- z pointing in the beam direction, with the beam rotating clockwise seen from above. Since the girders are straight no curvilinear system has to be defined as for the beam.

A girder may be displaced from its reference positions in six degrees of freedom:

- Sway, translation u along x-axis
- Heave, translation v along y-axis
- Surge, translation w along z-axis
- Pitch, rotation around around x-axis by angle χ
- Yaw, rotation around y-axis by angle η
- Roll, rotation around z-axis by angle σ

Sway, heave, pitch, yaw and roll are subject of dynamic alignment by means of the 5-point mover system. The surge (translation along z-axis) is suppressed by mechanical fixations only. Since surges are less critical for beam stability they had been omitted from dynamic control. The rotation angles χ, η, σ are positive when the rotation is counter clockwise as seen from the positive side of the corresponding axis. We thus get for the rotations:

$$\text{Pitch (around } x\text{):} \quad R_x = \begin{pmatrix} 1 & 0 & 0 \\ 0 & \cos\chi & -\sin\chi \\ 0 & \sin\chi & \cos\chi \end{pmatrix} \tag{1}$$

$$\text{Yaw (around } y\text{):} \quad R_y = \begin{pmatrix} \cos\eta & 0 & \sin\eta \\ 0 & 1 & 0 \\ -\sin\eta & 0 & \cos\eta \end{pmatrix} \tag{2}$$

$$\text{Roll (around } z\text{):} \quad R_z = \begin{pmatrix} \cos\sigma & -\sin\sigma & 0 \\ \sin\sigma & \cos\sigma & 0 \\ 0 & 0 & 1 \end{pmatrix} \tag{3}$$

Multiplication gives the full rotation matrix

$$R = R_z R_y R_x = \begin{pmatrix} \cos\sigma\cos\eta & \cos\sigma\sin\eta\sin\chi - \sin\sigma\cos\chi & \cos\sigma\sin\eta\cos\chi + \sin\sigma\sin\chi \\ \sin\sigma\cos\eta & \sin\sigma\sin\eta\sin\chi + \cos\sigma\cos\chi & \sin\sigma\sin\eta\cos\chi - \cos\sigma\sin\chi \\ -\sin\eta & \cos\eta\sin\chi & \cos\eta\cos\chi \end{pmatrix} \tag{4}$$

Of course, the determinant of the rotation matrix is unity: $|R| = 1$. A linearized rotation matrix is obtained by assuming $\chi, \eta, \sigma \ll 1$ and neglecting all orders higher than linear in R:

$$R_{\text{lin}} = \begin{pmatrix} 1 & -\sigma & \eta \\ \sigma & 1 & -\chi \\ -\eta & \chi & 1 \end{pmatrix} \tag{5}$$

The determinant deviates from unity in second order of the angles: $|R_{\text{lin}}| = 1 + \chi^2 + \eta^2 + \sigma^2$. R_{lin} is independent of the order of the multiplications whereas R is not.

The translations and the rotations may be conveniently combined into vectors:

$$\vec{t} = \begin{pmatrix} u \\ v \\ w \end{pmatrix} \qquad \vec{\theta} = \begin{pmatrix} \chi \\ \eta \\ \sigma \end{pmatrix} \tag{6}$$

Transformation from an ideal vector $\vec{x_o}$ into a displaced vector $\vec{x}$ is given by

$$\vec{x} = R(\vec{x_o} + \vec{t}) \tag{7}$$

In case of linear approximation (which will be used frequently) this equation reduces to

$$\vec{x} = R_{\text{lin}}\vec{x_o} + \vec{t} \tag{8}$$

neglecting the second order terms from the product $R_{\text{lin}}\vec{t}$. Using eqs.5,6 we may also write

$$\vec{x} = \vec{x}_o + \vec{\theta} \times \vec{x}_o + \vec{t} \tag{9}$$

or explicitly

$$\begin{pmatrix} x \\ y \\ z \end{pmatrix} = \begin{pmatrix} x_o - \sigma y_o + \eta z_o + u \\ y_o - \chi z_o + \sigma x_o + v \\ z_o - \eta x_o + \chi y_o + w \end{pmatrix} \tag{10}$$

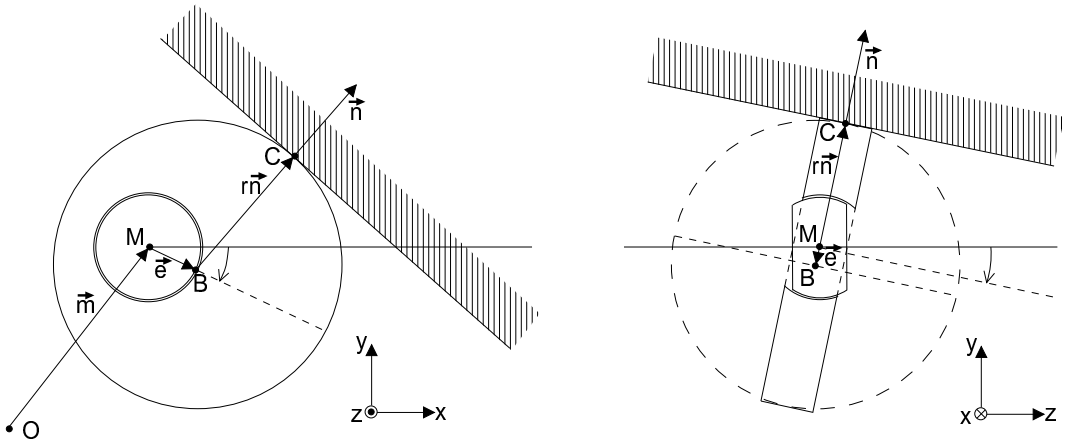

Figure 1: Schematic view of girder mover 1

3 The girder mover system

Since the girder mover system has no control of surges w (which are less relevant for beam dynamics) we set $w \equiv 0$ during this section and use eq.6 and the subsequent equations with this restriction.

The girder mover system is based on five motor-driven excentric disks oriented in z-direction which support five contact surfaces of the girder. As shown in figures 4, four of the five surface are slanted by 45° and one is horizontal.

Figure 1 shows exaggerated the girder mover 1 from figure 4: It consists of an axis located at point M with the motor drive attached to it and an excentric disk touching the girder's contact surface. The ball bearings between axis and disk allow some rotation around the x-axis in order to avoid localized pressure on the disk edges, they thus create a virtual sphere of radius r centered at point B.

The vector $\vec{m}$ points to the axis at point M. This notation will be used for all points. $\vec{m}$ is rigid and given by the geometric layout. Data for the SLS girders are given in table 1.

The vector $\vec{e}$ points in the direction of the waist (maximum radius) of the excentric disk. ϕ is the rotation angle of the axis, i.e. the inclination between $\vec{e}$ and the x-axis. Since the excenter can only rotate in the

Table 1: Geometric data for SLS girder movers

Girder mover	No.	1	2	3	4	5
Midpoint of motor axis	m_x [mm]	-410	$+410$	$+410$	-344	-476
	m_y [mm]	-602	-602	-602	-602	-602
	m_z [mm]	$-g$	$-g$	$+g$	$+g$	$+g$
		for g see table 3				
Radius of motor axis	e	5	5	5	5	5
Radius of excentric disk	r	60	60	60	60	60
Excenter ideal angle	ϕ_o	$-45°$	$-135°$	$0°$	$-135°$	$-45°$
Contact surface ideal angle	ψ_o	$45°$	$135°$	$90°$	$135°$	$45°$
constants for eq.24	c	1	-1	0	-1	1
	s	1	1	$\sqrt{2}$	1	1
	p	-1	1	-1	1	-1

$x-y$ plane, in the ideal case (no distortions) the vector $\vec{e}_o$ is given by

$$\vec{e}_o = e \begin{pmatrix} \cos\phi_o \\ \sin\phi_o \\ 0 \end{pmatrix} \tag{11}$$

e is the radius of the axis, i.e. the distance between motor axis M and virtual ball midpoint B.

$\vec{n}$ is the normal vector of the planar contact surface. $-\vec{n}$ always points to point B. $\vec{n}$ of course is affected by the girder misalignments $(u, v, \chi, \eta, \sigma)$. For the ideal case it is given by

$$\vec{n}_o = \begin{pmatrix} \cos\psi_o \\ \sin\psi_o \\ 0 \end{pmatrix} \tag{12}$$

since (in the ideal case, where $\chi = 0$) it has no z-component.

C is the point of contact between excenter disk and girder contact surface:

$$\vec{c} = \vec{m} + \vec{e} + r\vec{n} \tag{13}$$

A defines any point in the contact plane required later to test other points on wether they are in the contact surface. For convenience we choose the ideal contact point for this vector:

$$\vec{a}_o = \vec{c}_o \tag{14}$$

Later due to misalignments and according to eq.7 this point will move away and will not coincide with the contact point anymore:

$$\vec{a} \neq \vec{c} \tag{15}$$

Table 1 gives data for the SLS girders (also see fig. 4).

3.1 Exact calculation of excenter angles

We will now calculate exactly the rotation angle of the excenters for given vectors $\vec{a}$ and $\vec{n}$ determined by the girder geometry and misalignment.

The excenter has contact to the surface if C is a point in the surface plane:

$$(\vec{c} - \vec{a}) \cdot \vec{n} = 0 \tag{16}$$

The contact vector, as seen from the excenter's side, was given by eq.13 As long as there is no pitch the excenter vector appearing in eq.13 is given by eq.11 as to be seen from figure 1. However the pitch of the girder tilts the excentric disk, thus the rotation from eq.1 has to be applied:

$$\vec{e} = R_x \vec{e_o} = e \begin{pmatrix} \cos\phi \\ \sin\phi\cos\chi \\ \sin\phi\sin\chi \end{pmatrix} \tag{17}$$

Yaw and roll do not tilt the disk in its bearings but just rotate it, which does not affect the excenter vector. Since e is a few mm and χ in the few mrad range, the pitch of the excenter will have virtually no effect. We only include it for exactness of the solution. Inserting eqs.13,17 into 16 we thus get

$$n_x \cos\phi + \underbrace{(n_y \cos\chi + n_z \sin\chi)}_{:=\tilde{n}_y} \sin\phi = \underbrace{-\frac{(\vec{m} - \vec{a}) \cdot \vec{n} + r}{e}}_{:=k} \tag{18}$$

The drive range for the excenter angle ϕ is $\pm 90°$ from maximum to minimum with the ideal position ϕ_o providing no shift defined as zero. In order to avoid ambiguities of trigonometric functions when crossing quadrant boundaries we subtract the initial angle by defining

$$\hat{\phi} = \phi - \phi_o \tag{19}$$

and modifying eq.18 subsequently:

$$\cos\hat{\phi}\underbrace{(n_x\cos\phi_o + \tilde{n}_y\sin\phi_o)}_{:=\hat{n}_x} + \sin\hat{\phi}\underbrace{(-n_x\sin\phi_o + \tilde{n}_y\cos\phi_o)}_{:=\hat{n}_y} = k \tag{20}$$

Substituting sine and cosine of $\hat{\phi}$ by tangens, squaring the equation and resubstituting eq. 19 we get for the exact solution of excenter angles

$$\phi = \phi_o + \arctan\left(\frac{-\hat{n}_x\hat{n}_y \pm k\sqrt{\hat{n}_x^2 + \hat{n}_y^2 - k^2}}{\hat{n}_y^2 - k^2}\right) \tag{21}$$

All quantities contained in eqs. 18-21 are known: $\vec{m}$, r, e are fixed quantities (constants), and $\vec{a}$, $\vec{n}$ are given by girder geometry and misalignments u, v, χ, η, σ. In the particular case of the SLS giders the positive root has to be taken for movers 1,3,5 and the negative root for 2 and 4. A negative argument of the square root indicates that the given girder misalignments are out of reach for the excenters. Note that eq.21 is generally valid since the SLS-specific simplifications from eqs.11 and 12 had not been used.

3.2 Linearized calculation of excenter angles

Since the range of girder motion as defined by the girder mover parameters is in the mm-range for the translations u, v and in the mrad-range for the rotations χ, η, σ, we may consider these value as small and treat the problem in linear approximation, i.e. neglecting second and higher orders of these values, in order to arrive at simpler formulae.

We apply the linearized rotation matrix R_{lin} from eq.5 and the translation from eq.6 to the vectors $\vec{a}_o$. To the surface normal vector $\vec{n}_o$ as defined by eq.12 we apply only the rotation since a normal vector is invariant to translations. Introducing the results into eq.18 we arrive at

$$\begin{aligned} &e\cos\phi(\cos\psi_o - \sigma\sin\psi_o) + e\sin\phi(\sin\phi_o + \sigma\cos\psi_o) = \\ &\quad\cos\psi_o(a_{xo} - m_x - \sigma m_y + \eta m_z + u) + \sin\psi_o(a_{yo} - m_y + \sigma m_x - \chi m_z + v) \end{aligned}$$

Vector $\vec{a}_o$ is taken from eqs.11-14 and its components substituted into the right hand side of the equation above. To the left hand side we apply trigonometry:

$$\text{l.h.s}/e = \cos(\phi - \psi_o) + \sigma\sin(\phi - \psi_0) \approx \cos(\phi - \psi_o - \sigma)$$

We thus get:

$$e\cos(\phi - \psi_o - \sigma) = \cos\psi_o(u - \sigma m_y + \eta m_z) + \sin\psi_o(v + \sigma m_x - \chi m_z) + e\cos(\phi_o - \psi_o) \tag{22}$$

From table 1 we see that for the particular case of the SLS girders the difference $(\phi_o - \psi_o)$ amounts to an odd multiple of 90° for all five girder movers, because the initial excenter position is orthogonal to the contact surface normal vector. Thus the last cosine term disappears and we get

$$\phi = \psi_o + \sigma \pm \arccos\left(\cos\psi_o\frac{u - \sigma m_y + \eta m_z}{e} + \sin\psi_o\frac{v + \sigma m_x - \chi m_z}{e}\right) \tag{23}$$

The $\pm$ sign takes into account the ambiguity of the arccos function and we have to use the right sign depending on the girder mover we consider. We further may substitute cosine and sine of ψ_o since these angles are known and constant. Using from table 1 the constants $c = \sqrt{2}\cos\psi_o$, $s = \sqrt{2}\sin\psi_o$ and the constant p taking into account the appropriate signs, and further exploiting the freedom to subtract 2π we finally arrive at an applicable simple formula for the 5 angles:

$$\phi_i = \psi_{oi} + \sigma + p_i \left[\arccos\left(\frac{c_i(u - \sigma m_{yi} + \eta m_{zi}) + s_i(v + \sigma m_{xi} - \chi m_{zi})}{\sqrt{2}e}\right) - \pi\right] - \pi \qquad i = 1\ldots 5 \tag{24}$$

The differences to the exact formula from eq.21 amount to less than 1° in the excenter angles ϕ. This corresponds to a few μm or μrad error only when recalculating the misalignments from the excenter angles as we will do in the next section.

3.3 Girder moving range

Figure 5 displays the linearized excenter angles according to eq.24 as functions of the five misalignments when only one of the misalignments is varied and the others kept zero. The maximum range of misalignments is reached when the argument of the arccos-function in eq.24 becomes ± 1. Written explicitly for the 5 girder movers with the data from table 1 we get 5 equations for the maximum values of the translations (in mm) and the angles (in rad), with $g = 1000$ for the short girder and $g = 1400$ for the long girder according to table 3:

$$\begin{array}{lrcl}
\text{GM1:} & |u + v + g\chi - g\eta + 192\,\sigma| & = & 5\sqrt{2} \\
\text{GM2:} & |-u + v + g\chi + g\eta - 192\,\sigma| & = & 5\sqrt{2} \\
\text{GM3:} & |v - g\chi + 410\,\sigma| & = & 5 \\
\text{GM4:} & |-u + v - g\chi - g\eta - 946\,\sigma| & = & 5\sqrt{2} \\
\text{GM5:} & |u + v - g\chi + g\eta + 126\,\sigma| & = & 5\sqrt{2}
\end{array} \tag{25}$$

If only one of the misalignments is activated we get a table of ranges:

Misalignment	Symbol	Range [$\pm$mm, $\pm$mrad]		Limiting GM
		short girder	long girder	
Sway	$u_{\max}$	7.07	7.07	1,2,4,5
Heave	$v_{\max}$	5.0	5.0	3
Pitch	$\chi_{\max}$	5.0	3.57	3
Yaw	$\eta_{\max}$	7.07	5.05	1,2,4,5
Roll	$\sigma_{\max}$	7.47	7.47	4

Of course, combinations of misalignments reduce the range: For example moving the girder along a line $x = y$ allows a maximum of ± 3.53 mm for u and v, reached when GM1 and GM4 are pressing their waists against the contact surfaces while GM2 and GM4 are doing nothing. The pitch χ corresponds to heave v and the yaw η to sway u with the mover pairs GM1/5 and GM2/4 working parallel for the translations and antiparallel for the rotations as clearly visible in figure 5. The roll motion is more complicated: For GM1,2,5 the surface normal vectors almost point to the beam axis, where the roll is defined (see figures 4), thus the girder is allowed to "roll" almost free on GM1,2,5 . Roll control is provided by GM3 and 4 essentially.

We may define a safe girder working region as 5-dimensional rectangular region unfolded by the 5 orthogonal intervals for independant variation of the misalignments. In the 2-dimensional case, for example if we consider u and v only, the working window is a rhomb which turns into a square-shaped rhomb if we normalize the coordinates to their maximum values from the table above: $\hat{u} := u/u_{\max}$. Obviously we get the maximum square area within limitations of $\hat{u}_{\lim} = \hat{v}_{\lim} = 1/2$.

The third row of equation 25 defines an octaeder, i.e. a 3-D rhomb, for v, χ and σ, whereas the other four rows define the equivalent of a rhomb in five dimensions[1]. From symmetry considerations we immediately see that we get $\hat{u}_{\rm lim} = 1/n$ etc. in case of an n-dimensional rhomb. From the five girder movers we thus get one cubical (GM3) and four hyper-hyper-cubical working regions. The common working region for all movers is most simply defined by the minimum of the five limitations from every mover and given in the table below. Note that this common working region happens to be defined by GM4 alone. Also note that it is not necessarily the largest possible common working region.

Misalignment	Symbol	Range [±mm, ±mrad]	
		short girder	long girder
Sway	$u_{\rm lim}$	1.41	1.41
Heave	$v_{\rm lim}$	1.41	1.41
Pitch	$\chi_{\rm lim}$	1.41	1.01
Yaw	$\eta_{\rm lim}$	1.41	1.01
Roll	$\sigma_{\rm lim}$	1.49	1.49

3.4 Calculation of girder displacements from excenter angles

Calculation of the excenter angles was done independently for each girder mover since the contact surface was given from the girder position status. If the surface was out of reach for the excenter no solution was found. For the opposite problem of finding the girder position for given excenter angles, in contrary the five angles will be correlated by the rigid girder. Further a solution will be found in any case since the girder has 5 degrees of freedom to follow the 5 movers. Since the girder position is found from a system of 5 coupled equations only a linear treatment can be done. The system is given from inversion of eq.24: The π-offsets and the sign constant $\hat{p}_i$ disappear in inversion since they were only constructed to resolve the ambiguity of the arccos-function. We further remember that $\sigma \ll 1$ and get:

$$M \cdot \vec{T} = \vec{q} \tag{26}$$

with $\vec{T}$ and $\vec{q}$ 5-dimensional vectors, $\vec{T}$ containing the misalignments we want to know,

$$\vec{T} = (u, v, \chi, \eta, \sigma),$$

and $\vec{q}$ containing the excenter angles:

$$q_i = \sqrt{2} e \cos(\phi_i - \psi_o) \qquad i = 1 \ldots 5$$

The row-vectors of the 5×5 matrix M are given by

$$\vec{M}_i = (c_i,\ s_i,\ -m_{zi} s_i,\ m_{zi} c_i,\ p_i) \qquad i = 1 \ldots 5$$

with

$$p_i = m_{xi} s_i - m_{yi} c_i - \sqrt{2} e \sin(\phi_i - \psi_{oi})$$

The first four column vectors of matrix M contain constants given in table 1. The $5^{\rm th}$-column vector $\vec{p}$ and the right hand side vector $\vec{q}$ contain the excenter angles. Eventually the alignments are simply given by

$$\vec{T} = M^{-1} \cdot \vec{q} \tag{27}$$

However the instruction set of the processing unit (SPS) to be used for controlling the excenter motors includes no matrix inversion procedure. Thus an explicit formula was derived from eq.27 by means of the

[1] a 5-D object consisting of 10 corners, 40 edges, 80 surfaces, 80 cells and 32 hypercells!

symbolic code MAPLE:

$$
\begin{aligned}
u &= -[\sqrt{2}(-p_5q_1 + 2p_5q_4 + p_5q_2 - p_4q_1 + p_4q_2 + q_5p_1 + q_4p_1 - 2p_4q_5 - q_5p_2 - q_4p_2) \\
&\quad +2(-q_3p_1 + p_3q_5 + q_3p_2 - p_3q_4 + p_3q_1 - p_5q_3 - p_3q_2 + p_4q_3)]/(4D) \\
v &= -[\sqrt{2}(q_5p_1 - p_4q_1 + q_4p_1 + q_5p_2 + q_4p_2 - p_5q_1 - p_5q_2 - p_4q_2) \\
&\quad +2(p_3q_4 + p_3q_1 - p_5q_3 + p_3q_2 - p_4q_3 + p_3q_5 - q_3p_1 - q_3p_2)]/(4D) \\
\chi &= -[\sqrt{2}(q_5p_1 - p_4q_1 + q_4p_1 + q_5p_2 + q_4p_2 - p_5q_1 - p_5q_2 - p_4q_2) \\
&\quad +2(-p_3q_4 + p_3q_1 + p_5q_3 + p_3q_2 + p_4q_3 - p_3q_5 - q_3p_1 - q_3p_2)]/(4gD) \\
\eta &= [\sqrt{2}(-p_4q_1 + q_5p_1 + q_4p_1 + 2p_4q_5 - q_5p_2 - q_4p_2 - p_5q_1 - 2p_5q_4 + p_5q_2 + p_4q_2) \\
&\quad +2(q_3p_2 + p_3q_4 - p_3q_2 - p_4q_3 - q_3p_1 - p_3q_5 + p_5q_3 + p_3q_1)]/(4gD) \\
\sigma &= [\sqrt{2}(q_5 + q_4) - 2q_3]/D \\
\text{with} & \\
D &= \sqrt{2}(p_5 + p_4) - 2p_3
\end{aligned}
$$

Figure 6 shows the misalignments as function of the excursion of a single excenter $(\phi - \phi_o)$ while the other excenters are at their ideal positions ϕ_o. Measurements on the real girder were carried out and confirmed that the girder moves as predicted [3].

4 Calculation of misalignments from survey data

The girder positions have to be measured by geodetic survey after installation as well as later on in order to control setting motions of the hall. The survey data will be used to calibrate the online position control systems HLS and HPS.

We assume that there are n monuments attached rigidly to each girder, their ideal positions $\vec{x}_{oi}$ $(i = 1 \ldots n)$ are known, and their displaced positions $\acute{\vec{x}}_i$ are measured during survey. From the differences of measured to ideal positions we will now derive the girder misalignments. We further assume that every measurement $\acute{\vec{x}}_i$ is accompanied by an individual vector of errors $(\delta x_i, \delta y_i, \delta z_i)$.

Unlike in the previous sections we do no longer exclude a surge error w that could be caused through mounting the girder but is out of control for the excenters. We thus use the full translation and rotation vectors as defined in eq.6.

The problem of fitting linear model parameters, i.e. the girder misalignments, to a number of measurements with errors, i.e. the monuments, is treated by the standard procedure of linear least square minimization. It will give us the misalignment parameters with error estimates and the probability for the validity of the result as described in [4]:

$$\sum_{i=1}^{n} \left(\frac{\acute{x}_i - x_i}{\delta x_i}\right)^2 + \left(\frac{\acute{y}_i - y_i}{\delta y_i}\right)^2 + \left(\frac{\acute{z}_i - z_i}{\delta z_i}\right)^2 \longrightarrow \text{ min} \tag{28}$$

The estimate vectors $\vec{x}_i$ are given by applying the transformation from eq.7 to the ideal positions $\vec{x}_{oi}$ using the error vectors from eq.6. Since the six girder misalingments are linearly independant, eq.28 falls apart into six equations for the partial derivatives, e.g.

$$\frac{\partial \sum(\ldots)}{\partial u} = -2 \sum_{i=1}^{n} \frac{(\acute{x}_i - x_i)}{\delta x_i^2} \frac{\partial x_i}{\partial u} + \ldots = 0 \qquad \text{etc.}$$

The following calculation is straightforward: Assuming small misalignments we use the linear, explicit transformation from eq.10, do the differentation, extract the six misalignment parameters and write the six

equations as a 6×6 linear system:

$$\underbrace{\begin{pmatrix} N & K \\ K^T & L \end{pmatrix}}_{:=M} \cdot \underbrace{\begin{pmatrix} \vec{t} \\ \vec{\theta} \end{pmatrix}}_{:=\vec{T}} = \underbrace{\begin{pmatrix} \vec{c} \\ \vec{d} \end{pmatrix}}_{:=\vec{B}} \tag{29}$$

The 3×3 submatrices are given by (we omit the summation index i):

$$N = \begin{pmatrix} \sum \frac{1}{\delta x^2} & 0 & 0 \\ 0 & \sum \frac{1}{\delta y^2} & 0 \\ 0 & 0 & \sum \frac{1}{\delta z^2} \end{pmatrix} \qquad K = \begin{pmatrix} 0 & \sum \frac{z_o}{\delta x^2} & -\sum \frac{y_o}{\delta x^2} \\ -\sum \frac{z_o}{\delta y^2} & 0 & \sum \frac{x_o}{\delta y^2} \\ \sum \frac{y_o}{\delta z^2} & -\sum \frac{x_o}{\delta z^2} & 0 \end{pmatrix}$$

$$L = \begin{pmatrix} \sum \frac{y_o^2}{\delta z^2} + \frac{z_o^2}{\delta y^2} & -\sum \frac{x_o y_o}{\delta z^2} & -\sum \frac{x_o z_o}{\delta y^2} \\ -\sum \frac{x_o y_o}{\delta z^2} & \sum \frac{x_o^2}{\delta z^2} + \frac{z_o^2}{\delta x^2} & -\sum \frac{y_o z_o}{\delta x^2} \\ -\sum \frac{x_o z_o}{\delta y^2} & -\sum \frac{y_o z_o}{\delta x^2} & \sum \frac{x_o^2}{\delta y^2} + \frac{y_o^2}{\delta x^2} \end{pmatrix}$$

and the right hand side subvectors contain the measurements:

$$\vec{c} = \begin{pmatrix} \sum \frac{\acute{x} - x_o}{\delta x^2} \\ \sum \frac{\acute{y} - y_o}{\delta y^2} \\ \sum \frac{\acute{z} - z_o}{\delta z^2} \end{pmatrix} \qquad \vec{d} = \begin{pmatrix} \sum \frac{\acute{z} y_o}{\delta z^2} - \frac{\acute{y} z_o}{\delta y^2} + y_o z_o \left(\frac{1}{\delta y^2} - \frac{1}{\delta z^2} \right) \\ \sum \frac{\acute{x} z_o}{\delta x^2} - \frac{\acute{z} x_o}{\delta z^2} + z_o x_o \left(\frac{1}{\delta z^2} - \frac{1}{\delta x^2} \right) \\ \sum \frac{\acute{y} x_o}{\delta y^2} - \frac{\acute{x} y_o}{\delta x^2} + x_o y_o \left(\frac{1}{\delta x^2} - \frac{1}{\delta y^2} \right) \end{pmatrix}$$

In case of identical errors δ_i for all dimensions the right hand side vectors could be written nicely as

$$\vec{c} = \sum \frac{\acute{\vec{x}} - \vec{x}_o}{\delta^2} \qquad \vec{d} = \sum \frac{\vec{x}_o \times \acute{\vec{x}}}{\delta^2}$$

The alignment vector $\vec{T} = (\vec{t}, \vec{\theta})$ then is obtained from

$$\vec{T} = M^{-1} \vec{B}$$

The variances of the alignment vector components are given by the diagonal elements of the inverse matrix (covariance matrix):

$$(\delta T_i)^2 = M_{ii}^{-1} \quad \longrightarrow \quad \delta u = \sqrt{M_{11}^{-1}} \quad \text{etc.}$$

The quality of the fit is expressed by the value of the sum (also referenced to as χ^2) from eq.28 when inserting the fitted parameters, and a probability for the validity of the fit can be derived. For details see [4].

Note: If the survey data are measured in the global coordinate system, all vectors have to be transformed into the girders system by the inverse of eq. 41. This is incorrectly done for the vector of individual errors $(\delta x_i, \delta y_i, \delta z_i)$ since it actually contains no lengthes but the radii of an error ellipsoid. The rotational part of the transformation then creates a sheared ellipsoid of correlated errors in the girder's system. In case of identical errors δ_i for all dimensions the transformation is correct.

5 Misalignments of the bending magnets

The SLS bending magnet are located between girders and supported by a three point bearing. We will calculate now how the misalignments of the girders translate into a misalignment of the bend between.

For the TRACY [6] beam dynamics model we only need sway, heave and roll, but for completeness we will calculate surge, pitch and yaw too. The derivation is similar to obtaining the girder misalignments from excenter angles since both are problems of a rigid body supported by several balls.

We define a coordinate system of the bending magnet with the x-axis pointing in direction of the sagitta, the z-axis along the line connecting the ideal points where the beam enters and leaves the bend, and the y-axis pointing up, i.e. in field direction. The beam does not travel through the origin of this coordinate system but through a point with coordinates of (sagitta, 0,0) as shown in figure 2.

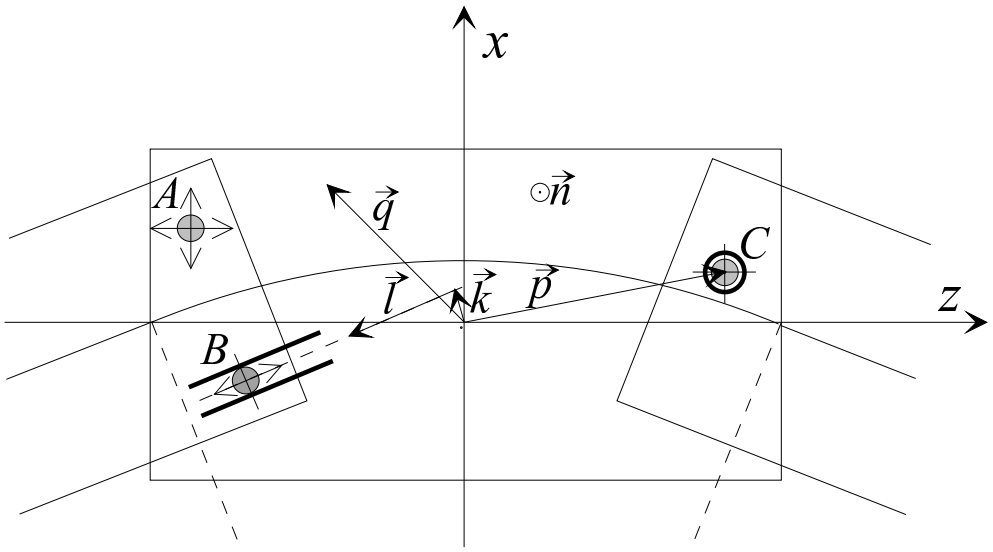

Figure 2: Three point bearing of bending magnet on two girders

The bend is supported by three bearings and held down to the bearings by its weight. The bearings are balls of 40 mm diameter creating [virtual] contact points to the bends bottom plane. Bearings A and B are on the upstream girder, bearing C downstream. The bearings are fixed rigidly to the girders and allow different degrees of freedom on the bend side: C is a cone providing a circular line of contact with the ball and thus creates a virtual contact point allowing no translations. A is just a surface and allows 2-dimensional freedom of motion. At B is a grove in the bend and allows translation only along its direction. Thus the bend's position is uniquely defined.

With $\vec{a}$,$\vec{b}$,$\vec{c}$ the midpoints of the balls in the bends coordinate system and r the ball radius we may express the constraints from the bearings in three equations:

A: contact to a flat surface. The contact point is given by $\vec{a} + r\vec{n}$ with yet unknown normal vector $\vec{n}$ of the bending magnets bottom plane. $\vec{q}$ is any point of that plane.

$$(\vec{a} + r\vec{n} - \vec{q}) \cdot \vec{n} = 0 \tag{30}$$

B: contact to a line in the bend's bottom plane defined by any point $\vec{k}$ of the line and its normal vector $\vec{l}$. The scalar λ gives the location along the line where the contact occurs:

$$\vec{b} + r\vec{n} = \vec{k} + \lambda\vec{l} \tag{31}$$

C: contact to a point and, with $\vec{p}$ the contact point on the bending magnets side, simply given by

$$\vec{c} + r\vec{n} = \vec{p} \tag{32}$$

With the scaler equation 30 and the two vector equations 31 and 32 we thus have seven equations for seven unknown quantities: The bend's misalignments u, v, w, χ, η, σ and the parameter λ which we don't need but we get it free.

All the vectors defined by the bending magnet are given by their ideal values we know and the misalignment transformation as given by eq.7. In the next step we apply the inverse transformation $\vec{x}_o = R^{-1}\vec{x} - \vec{t}$ to all vectors, i.e. we move into the misaligned bend's coordinate system (only the rotation is applied to the normal vectors):

$$\text{A:} \qquad (R^{-1}\vec{a} - \vec{t} + r\vec{n}_o - \vec{p}_o) \cdot \vec{n}_o = 0 \tag{33}$$

$$\text{B:} \qquad R^{-1}\vec{b} - \vec{t} + r\vec{n}_o = \vec{k}_o + \lambda\vec{l}_o \tag{34}$$

$$\text{C:} \qquad R^{-1}\vec{c} - \vec{t} + r\vec{n}_o = \vec{p}_o \tag{35}$$

We identify $\vec{p}_o = \vec{c}_o + r\vec{n}_o$ since this is just ideal contact point for bearing C. In the same way we use the freedom to choose $\vec{q}_o$ and $\vec{k}_o$ anywhere in the plane resp. in the grove to identify them with $\vec{a}_o + r\vec{n}_o$ and $\vec{b}_o + r\vec{n}_o$ resp. Thus we get

$$\text{A:} \qquad R^{-1}\vec{a} \cdot \vec{n}_o - \vec{t} \cdot \vec{n}_o = \vec{a}_o \cdot \vec{n}_o \tag{36}$$

$$\text{B:} \qquad R^{-1}\vec{b} - \vec{t} - \lambda\vec{l}_o = \vec{b}_o \tag{37}$$

$$\text{C:} \qquad R^{-1}\vec{c} - \vec{t} = \vec{c}_o \tag{38}$$

Introducing the inverse of the linear rotation matrix from eq. 5 and the misalingment vectors $\vec{t}$ and $\vec{\theta}$ from eq.6 we finally can write these seven equations as linear system:

$$\begin{pmatrix} 0 & n_{xo} & n_{yo} & n_{zo} & [\vec{a}\times\vec{n}_o]_x & [\vec{a}\times\vec{n}_o]_y & [\vec{a}\times\vec{n}_o]_z \\ l_{ox} & 1 & 0 & 0 & 0 & b_z & -b_y \\ l_{oy} & 0 & 1 & 0 & -b_z & 0 & b_x \\ l_{oz} & 0 & 0 & 1 & b_y & -b_x & 0 \\ 0 & 1 & 0 & 0 & 0 & c_z & -c_y \\ 0 & 0 & 1 & 0 & -c_z & 0 & c_x \\ 0 & 0 & 0 & 1 & c_y & -c_x & 0 \end{pmatrix} \cdot \begin{pmatrix} \lambda \\ u \\ v \\ w \\ \chi \\ \eta \\ \sigma \end{pmatrix} = \begin{pmatrix} (\vec{a} - \vec{a}_o)\cdot\vec{n}_o \\ b_x - b_{ox} \\ b_y - b_{oy} \\ b_z - b_{oz} \\ c_x - c_{ox} \\ c_y - c_{oy} \\ c_z - c_{oz} \end{pmatrix} \tag{39}$$

In beam dynamics studies on misaligments this rather complex calculation would be executed rather frequently. On the other hand only sway, heave and roll have a first order effect on the beam, where in case of the SLS storage ring using only gradient free rectangular bending magnets, sway does not affect the beam at all.

In order to simplify eq. 39 we first make use of the SLS specific geometric features that $l_{oy} = 0$ and $\vec{n}_o = (0, 1, 0)$. Then the program MAPLE was used to generate explicit and exact expressions for heave and roll:

$$\begin{aligned} v &= -(-a_z c_y b_x + a_z b_y c_x + a_x c_y b_z + a_x c_z b_{oy} - a_x c_z b_y - a_{oy} c_z b_x + a_y c_z b_x + b_x a_z c_{oy} \\ &\quad -a_y b_z c_x + a_{oy} b_z c_x - b_{oy} a_z c_x - a_x b_z c_{oy})/D \\ \sigma &= (-b_z a_y + b_z c_y + b_z a_{oy} + c_z b_{oy} - b_z c_{oy} - c_z b_y - \\ &\quad -a_z b_{oy} + a_z c_{oy} - a_z c_y + a_z b_y + c_z a_y - c_z a_{oy})/D \end{aligned}$$

with

$$D = -b_z a_x + b_z c_x - a_z c_x + a_z b_x - c_z b_x + c_z a_x$$

Note: The vectors $\vec{a}$,$\vec{b}$,$\vec{c}$ are defined in the bending magnet's coordinate system, but they are affected by the misalingments of the adjacent girders supporting the bending magnet. Thus several transformations have to be done using eqs. 8,41 in order to move from the bending magnet's system to the global system, from there to the girder's system, apply the misalignment and move back to the bending magnet's system.

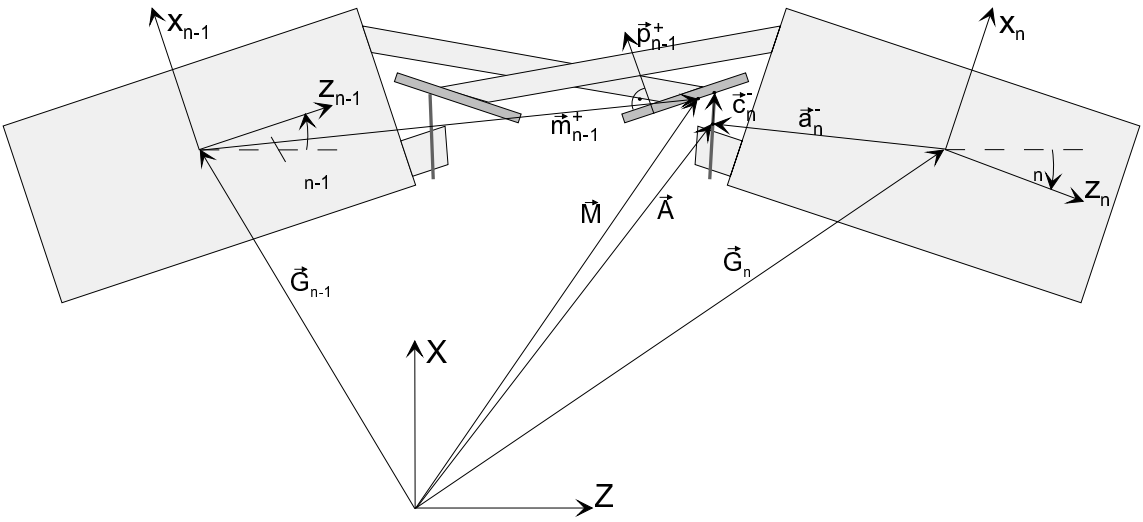

Figure 3: Principle of the horizontal positioning system

6 Girder position monitoring systems

The hydrostatic leveling system (HLS) and the horizontal positioning system (HPS) continuously monitor the movements of the girders. While the HLS, based on communicating tubes connected all around the machine, uses gravity as an absolute reference for vertical positions, the HPS, due to lack of a comparable reference in the horizontal, measures only relative movements between two girders or between a girder and a monument.

The third system at the SLS storage ring, the BPM position monitoring system (POMS) for online compensation of thermal and other drifts of the beam position monitors relative to the girders, is beyond the scope of this note [7].

6.1 The hydrostatic leveling system

Four HLS sensors, which are basically water pots with capacitive readouts, are mounted on every girder at locations given in table 2. They allow to determine heave, pitch and roll of the girder. Three sensor would be sufficient, the fourth one is redundant to cover failures and increase precision.

The formula to obtain heave, pitch and roll from HLS sensor signals is immediately extracted from the previous calculation of all six girder misalignments from survey data: In eq. 29 we simply omit all even numbered columns and rows which are related to sway, surge and yaw and get:

$$\begin{pmatrix} \sum \frac{1}{\delta^2} & -\sum \frac{z_o}{\delta^2} & \sum \frac{x_o}{\delta^2} \\ -\sum \frac{z_o}{\delta^2} & \sum \frac{z_o^2}{\delta^2} & -\sum \frac{x_o z_o}{\delta^2} \\ \sum \frac{x_o}{\delta^2} & -\sum \frac{x_o z_o}{\delta^2} & \sum \frac{x_o^2}{\delta^2} \end{pmatrix} \cdot \begin{pmatrix} v \\ \chi \\ \sigma \end{pmatrix} = \begin{pmatrix} \sum \frac{\Delta y'}{\delta^2} \\ -\sum \frac{z_o \Delta y'}{\delta^2} \\ \sum \frac{x_o \Delta y'}{\delta^2} \end{pmatrix} \tag{40}$$

$\Delta y'$ are the measured differences relative to the ideal machine level. δ are the individual sensor errors.

6.2 The horizontal positioning system

Figure 3 shows the principle of the horizontal positioning system: Two adjacent girders are connected by pairs of lever arms mounted underneath the bending magnet. From each girder a bolt is pressed against the

Table 2: Data for the position measurement systems

Geometric data of HLS system [mm]:

	x	y	z
sensor locations	± 410	–	$\pm g$

Geometric data of HPS system [mm]:

		x	y	z
sensor bolt origin	$\vec{a}_o^{\pm}$	x_a	$y^{\pm}$	$\pm(g + z_a)$
sensor bolt direction	$\vec{c}_o^{\pm}$	$\cos\phi^{\pm}$	0	$-\sin\phi^{\pm}$
contact plate location	$\vec{m}_o^{\pm}$	x_m	$y^{\pm}$	$\pm(g + z_m)$
contact plate normal	$\vec{p}_o^{\pm}$	1	0	0

with g from table 3 and the other constants depending on location:

girder number	n mod 4	$2^+, 3^-$	$1^+, 2^-, 3^+, 4^-$	$1^-, 4^+$
gap type:		wide	narrow	endpoint*
	$\phi^{\pm}$	$\mp 7°$	$\mp 4°$	-180°
	x_a	54.495	30.805	-405.0
	x_m	-43.0	-25.0	–
	z_a	917.192	611.828	715.0
	z_m	861.229	559.879	–
	y^-	-457.0	-457.0	-322.0
	y^+	-490.0	-490.0	-322.0

*Exceptions for 1^- and 48^+: $\phi = 0°$ and $x_a = +405.0$

contact plane at the end of the lever arm fixed to its neighbour. The elongation of the bolt is measured by means of an optical sensor with micrometer resolution over a range of several millimeters [7]. Either all girders around the machine may be linked in this way ("full train link") or only groups of girders are linked ("partial train link") with monuments terminating the train at its ends. In case of SLS groups of four girders extending over one of the 12 TBAs form partial trains.

We now will calculate how to obtain sway and yaw for all girders from the readouts of the HPS sensors: Since we consider correlations between girders we have to move into the "global" SLS coordinate system (X, Y, Z) with the origin at the center of the SLS hall (We will use capital letter to identify vectors in the global coordinate system). With $\vec{G}_n$ the midpoint of girder n and Φ_n its angle of orientation (i.e. the angle between beam and Z-axis) the transformation from local to global coordinates is given by

$$\vec{X} = \vec{G}_n + F_n \vec{x}_n \quad \text{with} \quad F_n = \begin{pmatrix} \cos\Phi_n & 0 & \sin\Phi_n \\ 0 & 1 & 0 \\ -\sin\Phi_n & 0 & \cos\Phi_n \end{pmatrix} \tag{41}$$

Data for SLS girder midpoints and orientations are given in table 3.

The contact from the sensor bolt to the contact plate of the adjacent girder is shown in figure 3: With $\vec{A}$ a point on the sensor bolt, $\vec{C}$ the normal vector of its direction as determined by the fixation allowing elongation as the only degree of freedom, $\vec{M}$ any vector in the contact plane and $\vec{P}$ the normal vector of the contact plane, we find for the condition of contact

$$(\vec{A} + \gamma\vec{C} - \vec{M}) \cdot \vec{P} = 0 \tag{42}$$

with γ the elongation of the bolt, i.e. the readout of the HPS sensor. It is important to note, that $\vec{A}$ and $\vec{C}$

move with girder n whereas $\vec{M}$ and $\vec{P}$ move with girder $n-1$. Eq. 42 is exact and makes neither use of linearization nor of SLS specific geometric data.

For the ideal case the HPS should give zero readings, i.e. $\gamma_o = 0$ and $\vec{A}_o = \vec{M}_o$, i.e.the vectors $\vec{A}_o$ and $\vec{M}_o$ are defined to coincide for the ideal case. Thus the corresponding vectors in the local coordinate systems are related by

$$\vec{G}_{n-1} + F_{n-1}\vec{m}_{n-1,o} = \vec{G}_n + F_n\vec{a}_{n,o} \tag{43}$$

In order to derive girder misalignments from HPS readouts we have to calculate the inverse of eq.42. Since the misalingments are small we will linearize eq.42 in order to become able to invert it and set

$$\gamma = d\gamma|_o \text{ since } \gamma_o = 0$$

Most terms of the total differential at "0" disappear due to $(\vec{M}_o - \vec{A}_o) = 0$ and we get

$$\gamma = \frac{(d\vec{M}|_o - d\vec{A}|_o)\cdot\vec{P}_o}{\vec{C}_o\cdot\vec{P}_o}$$

Now we insert the transformation from local coordinates according to eq.41. The origin vectors $\vec{G}$ disappear under differentiation; to the normal vectors they aren't applied anyway:

$$\gamma_n^{\pm} = \frac{(F_{n\pm1}d\vec{m}_{n\pm1}^{\mp}|_o - F_n d\vec{a}_n^{\pm}|_o)\cdot F_{n\pm1}\vec{p}_{n\pm1,o}^{\mp}}{F_n\vec{c}_{n,o}^{\pm}\cdot F_{n\pm1}\vec{p}_{n\pm1,o}^{\mp}} \tag{44}$$

Here we have written two equations in one because every girder has *two* sensors at its upstream (-) and downstream (+) ends: The contact plate vectors $\vec{m}_{n-1}^{+}$, $\vec{p}_{n-1}^{+}$ on the *downstream* end of the *upstream* girder $n-1$ and the sensor bolt vectors $\vec{a}_n^{-}$, $\vec{c}_n^{-}$ on the *upstream* side of girder n are involved in the measurement situation shown in figure 3.

Calculating the total differentials $d\vec{m}_{n\pm1}^{\mp}$ and $d\vec{a}_n^{\pm}$ with respect to all misalignments is equivalent to application of the linearized transformation from eq.8

$$d\vec{x} = \vec{x} - \vec{x}_o = (R-1)\vec{x}_o + \vec{t}$$

Since the scalar products are independant of the coordinate system we rotate into a system parallel to the upstream girder by multiplication with $F_{n\pm1}^{-1}$ in order to exploit the simple structure of the normal vector $\vec{p}^{\mp}$ as given in table 2:

$$\gamma_n^{\pm} = \frac{((R_{n\pm1}-1)\vec{m}_{n\pm1,o}^{\mp} + \vec{t}_{n\pm1} - F_{n\pm1}^{-1}F_n((R_n-1)\vec{a}_{n,o}^{\pm} + \vec{t}_n))\cdot\vec{p}_{n\pm1,o}^{\mp}}{F_{n\pm1}^{-1}F_n\vec{c}_{n,o}^{\pm}\cdot\vec{p}_{n\pm1,o}^{\mp}} \tag{45}$$

For the sensors between girders as installed under all bending magnets, the angles of orientation of the sensor bolt normal vectors are given by

$$\phi_n^{\pm} = \frac{\Phi_{n\pm1} - \phi_n}{2} \quad .$$

For the sensors at the ends of the train measuring position against fixed monuments they are given by

$$\phi_1^{-} = \phi_N^{+} = -\pi \quad .$$

Thus the transformations $F_{n\pm1}^{-1}F_n$ are rotations by $-2\phi^{\pm}$.

Now we insert the explicit transformations from eq.10 and the SLS specific values $c_{ox}^{\pm} = cos\phi^{\pm}$ and $p_{xo}^{\mp} = 1$, $p_{yo}^{\mp} = p_{zo}^{\mp} = 0$ from table 2 into eq.45:

$$\begin{aligned} u_{n\pm1} + m_{n\pm1,oz}^{\mp}\eta_{n\pm1} - C_n^{\pm}u_n - (C_n^{\pm}a_{n,oz}^{\pm} + S_n^{\pm}a_{n,ox}^{\pm})\eta_n = \\ \gamma_n^{\pm}\cos\phi_n^{\pm} + m_{n\pm1,oy}^{\mp}\sigma_{n\pm1} - C_n^{\pm}a_{n,oy}^{\pm}\sigma_n - S_n^{\pm}a_{n,oy}^{\pm}\chi_n - S_n^{\pm}w_n \end{aligned} \tag{46}$$

with

$$C_n^{\pm} = \cos(\phi_n^{\pm}) \qquad S_n^{\pm} = \sin(\phi_n^{\pm})$$

Introducing the constants given in table 2 we also may write for convenience

$$\begin{aligned} u_{n\pm1} \mp (g_{n\pm1} + z_{m,n\pm1})\,\eta_{n\pm1} - C_n^{\pm} u_n - (S_n^{\pm} x_{a,n} \pm C_n^{\pm}(g_n + z_{a,n}))\,\eta_n = \\ \gamma_n^{\pm}\cos\phi_n^{\pm} + y_{n\pm1}^{\mp}\sigma_{n\pm1} - C_n^{\pm} y_n^{\pm}\sigma_n - S_n^{\pm} y_n^{\pm}\chi_n - S_n^{\pm} w_n \end{aligned} \tag{47}$$

where the appropriate constants have to be chosen depending on the value of n.

The quantities $u_{n\pm1}, \eta_{n\pm1}, u_n, \eta_n$ on the left side are to be measured by the HPS, whereas the quantities $\sigma_{n\pm1}, \sigma_n, \chi_n, w_n$ on the right side disturb the measurements and thus have to be determined in advance by the HLS system. The surge w_n which is out of control for the girder movers anyway and thus hopefully never will change, is set to zero by initial HPS calibration.

Since tbe HPS sensors are mounted *under* the beam location (which is origin of the girder's coordinate system) the rolls of both girders show strong and opposite effects. Since the contact plate at $\vec{m}_o^{\mp}$ is oriented parallel to the adjacent girder's $(y_{n\pm1}, z_{n\pm1})$ plane, its heave $v_{n\pm1}$, pitch $\chi_{n\pm1}$ and surge $w_{n\pm1}$ cannot affect the values of $\gamma_n^{\pm}$. However seen from the other girder the contact plate is tilted by $\phi_n^{\pm}$ causing a slight influence from its own pitch χ_n and surge w_n. Only the heave v_n is suppressed since the plate is at least parallel to the y_n-axis.

Eqs. 46,47 also apply to the first (γ_1^-) and last (γ_N^+) girder of a partial train facing terminating monuments by setting the $n \pm 1$ indexed quantities to zero. Inserting all values for $n = 1 \ldots N$, eq. 46 or 47 forms a $2N$ dimensional linear system.

This system may be written as a 4-diagonal $2N \times 2N$ matrix multiplied with the $2N$ vector of horizontal misalignments as shown beside for $N = 4$. Only the shaded elements are nonzero. In case of a full circular train link also the cross-marked elements would be nonzero. Inversion of the matrix provides the unique solution of horizontal misalignments. However in case of a full train link the matrix becomes singular, probably this reflects the fact that in case of a full train link the whole machine is "floating" and unique solutions for the misalignments cannot be found. Replacing any of the links by two monuments again gives a unique solution.

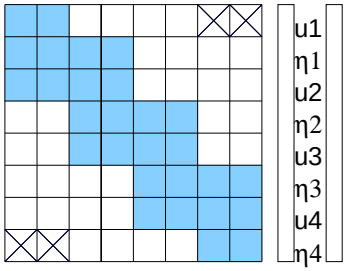

7 Beam based girder alignment

Correction of the beam orbit in the SLS storage ring is performed by adjusting each N=72 horizontal and vertical corrector magnets until the M=72 beam position monitors (BPM) return zero readings. The response matrix correlates the excitations of correctors to the BPM readings and may be derived from theory or measured with the beam. Its inverse is called the correction matrix, it correlates the BPM readings to the correctors, i.e. it tells how the correctors have to be excited in order to affect the reading of a single BPM. While the response matrix is covered everywhere with betatron oscillations, the correction matrix of a well designed orbit correction scheme is a tridiagonal matrix revealing the local bumps as used commonly in orbit correction. In the particular case of SLS both matrices are square matrices, however in general M may be larger or smaller than N leading to under- or overdetermined systems. Furthermore the system may be degenerate, i.e. the rank is reduced, if some correctors are linear combinations of others or don't work at all. That situation is treated best by the method of singular value decomposition (SVD), which is able to solve non-square systems in a least square sense for either the corrector strengthes ($M < N$) or the BPM readings ($M > N$), allows to "invert" non-square as well as singular matrices and returns a vector of weight factors indicating the efficiency of the different correctors. Very low weight factors expose useless

correctors which contain the risk to amplify noise and steer the system to extreme values. They will be set to zero in order to reduce the rank of the system to a smaller set of efficient correctors providing a robust even not complete solution [4].

This method had been applied to static and dynamic closed orbit correction in the SLS storage ring [5]. We will now apply it to beam based girder alignment by treating the girder misalignments like correctors. We define "correctors" as displacements of girder ends and thus get 96 horizontal and vertical correctors from 48 girders in SLS ($n = 1 \ldots 48$):

$$x_{2n-1} = u_n - L_n\eta_n/2 \quad x_{2n} = u_n + L_n\eta_n/2 \quad y_{2n-1} = v_n - L_n\chi_n/2 \quad y_{2n} = v_n + L_n\chi_n/2$$

L_n is the length of girder n. Girder rolls are omitted prelimarily. An excitation of the "corrector" will *somehow* affect the beam because it will pass the magnets on the girder off-axis and thus receive some kick. The correlated axis errors of magnets and BPMs due to girder misalignments were easily modelled thanks to the flexibility of the TRACY beam dynamics code [6], the response matrices were "measured" in simulation, and the correction matrices were obtained from SVD (SVD code from CERNLIB). The results are shown in figure 7: The response matrices show the betatron motions along the monitor axis and the lattice structure along the girder axis: Horizontal and vertical betatron tunes are 20.82 and 8.28 for SLS, and the lattice is a period three lattice composed of 12 TBA sectors. The correction matrices show a diagonal structure as expected. However compared to the classic corrector magnet based tridiagonal correction matrix as shown in [5], the girder correction matrix diagonal is diluted: more off-diagonal elements are involved, i.e. several more than three girders are required to correct the orbit in one particular BPM, or other speaking, local bumps extend over larger regions. This is due to the finite length of the girders, whereas the corrector magnets were treated as thin lenses.

Examination of the weight factors ω_i indicates some degeneracy in the horizontal: The lowest weight factor is only $3.7 \cdot 10^{-4}$ of the largest one. Probably the girders producing the pale bands of small numbers in the horizontal response matrix image of fig. 7 are inefficient due to betatron phase advances of $\approx$180° over a girder, leading to a linear dependancy of the two "correctors" corresponding to displacements of its ends. Note, that the average phase advance per girder already amounts to 156° in the horizontal. In the vertical the ratio of minimum to maximum weight factor is a moderate value of 0.013 and no degeneracy occurs.

For testing the beam based girder alignment, 200 random seeds for misalignments were generated and corrected: The application of random errors assumed partial train links over four girders (one sector) with an rms (cut at 2 sigma) displacement error of 300 μm for the [virtual] girder joints, 100 μm for the joint play (i.e. the precision of HLS and HPS systems) and 50 μm for the mounting of magnets and BPMs relative to the girder. No roll errors were applied and no misalignments of the bending magnets were set. No threader was used and 191 initial orbits were found.

As a first step the orbit correction was done in the classic way by excitation of the corrector magnets. 3 orbits were lost in this process, i.e. the orbit correction diverged.

In a second step the correctors were reset to zero while keeping the same set of random seeds, and the girder "correctors" were now used to correct the beam. Afterwards the corrector magnets were activated again to suppress any residual orbit left over from girder alingment. Finally the values of corrector strength from first step, i.e. without, and second step, i.e. with beam based girder alignment were compared. Results are shown in figure 8:

The procedure worked perfectly in the vertical: The correctors remained at zero strength after girder alignment, i.e. all static vertical closed orbit correction is fully covered by girder alignment! This is a very beneficial result since the maximum corrector strenghtes up to 0.6 mrad before girder alingment were already close to the correctors' capabilities (0.74 mrad at 2.4 GeV). There is little change in the

rms or maximum girder heave before and after corrections, however the individual values were exchanged completely moving from a random to an optimum pattern of misalignments. In the pitch we see a systematic fluctuation after alignment, obviously the pitch of girders in the TBAs was reduced and the pitch of girders at the straights was increased, leading to an increase of the maximum pitch occurring, but still well within the limits defined in section 3.3.

In the horizontal some more care was required:

- No filtering of weight factors, i.e. allowing the algorithm to use all 96 "correctors" (all 48 girders) resulted in switched off horizontal correctors too, however 16 of the 188 seeds were lost due to divergence of the correction loop. In reality this scheme would not be applicable since it is too sensitive to noise in BPM readings and to finite precision of girder alignment.
- Filtering the weight factors by the requirement $\omega_i > 0.01 \cdot \omega_{\max}$ left only 21 from 96 correctors. Consequently, no seed was lost, but the girder alignment was changed by very little amounts and no load was taken away from the corrector magnets.
- Filtering the weight factors by the requirement $\omega_i > 0.001 \cdot \omega_{\max}$ left 60 from 96 correctors. Again no seed was lost, but now the rms and maximum corrector magnet strength was reduced by a factor four by just reshuffling the girder misalingments while not or little increasing their rms and maximum sway and yaw. This case is shown in figure 8.

Beam based girder alignment is able to lower the corrector magnet strengthes significantly both horizontally and vertical. It thus may take over most of the static (DC) orbit correction and leave the corrector strength to dynamic correction (active orbit feedback) and local bump creation for matching to beamline acceptances or for machine studies. Since beam based girder alignment is a dynamic method and, in principle, may be done online with the stored beam, it appears to be a superior substitute for magnet sorting.

More detailed studies on beam based girder alignment are in progress. Basically it should be possible to optimize the emittance coupling by steering the roll motion of the girders. Also bending magnet misalingments will be included in further simulations. Results will be reported after commissioning of the SLS storage ring and testing the algorithm with real beam.

References

[1] M.Böge et al., The SLS accelerator complex: an overview, Proc. EPAC 98, p.623

[2] M.Böge et al., SLS lattice finalization and magnet girder design, Proc. EPAC 98, p.644

[3] P.Wiegand, SLS SR girder mover: Control system test, SLS-TME-TA-2000-0145, Jan. 2000

[4] W.H.Press et al, Numerical Recipes, Cambridge 1989

[5] M.Böge et al., Fast closed orbit correction in the SLS storage ring, Proc. PAC 99, p.1129

[6] M.Böge, Update on TRACY-2 documentation, Internal report SLS-TME-TA-1999-0002

[7] V.Schlott, Monitoring of mechanical drifts at SLS using linear encoders, PSI Annual Report 1998, Annex VII, p.19

[8] `http://slsbd.psi.ch/~ streun/dynal/`

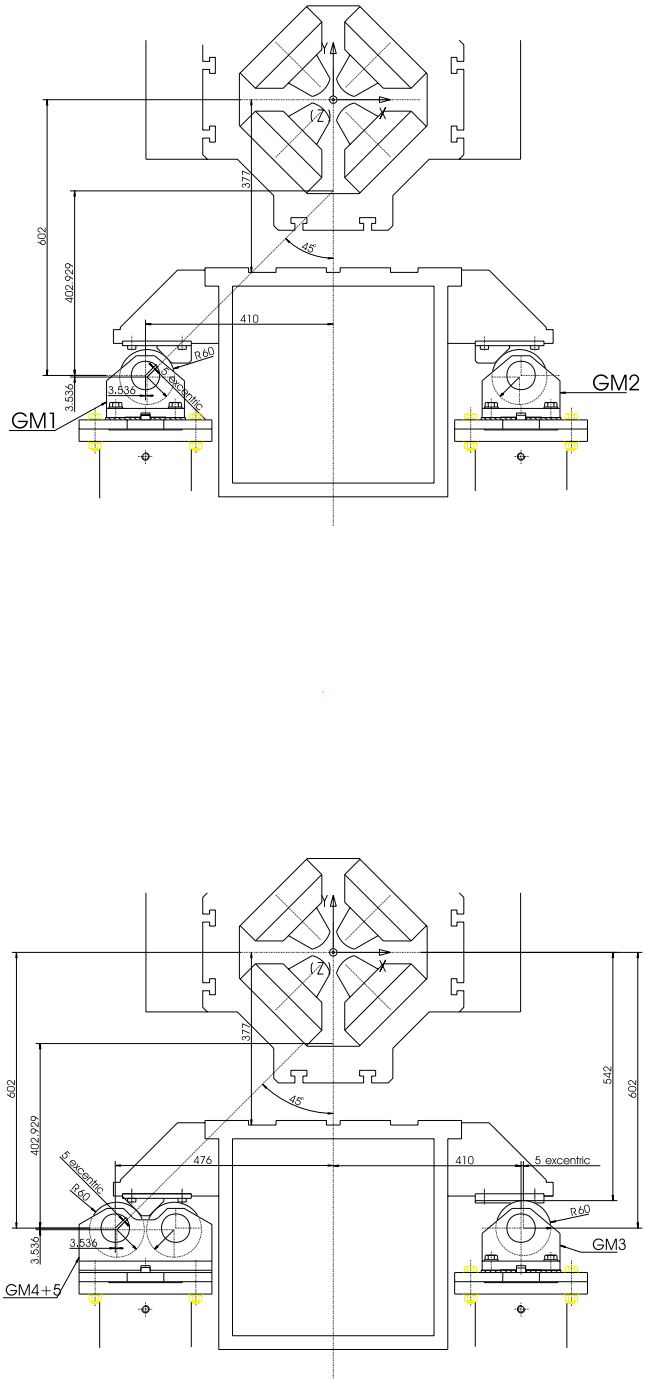

Figure 4: Girder movers

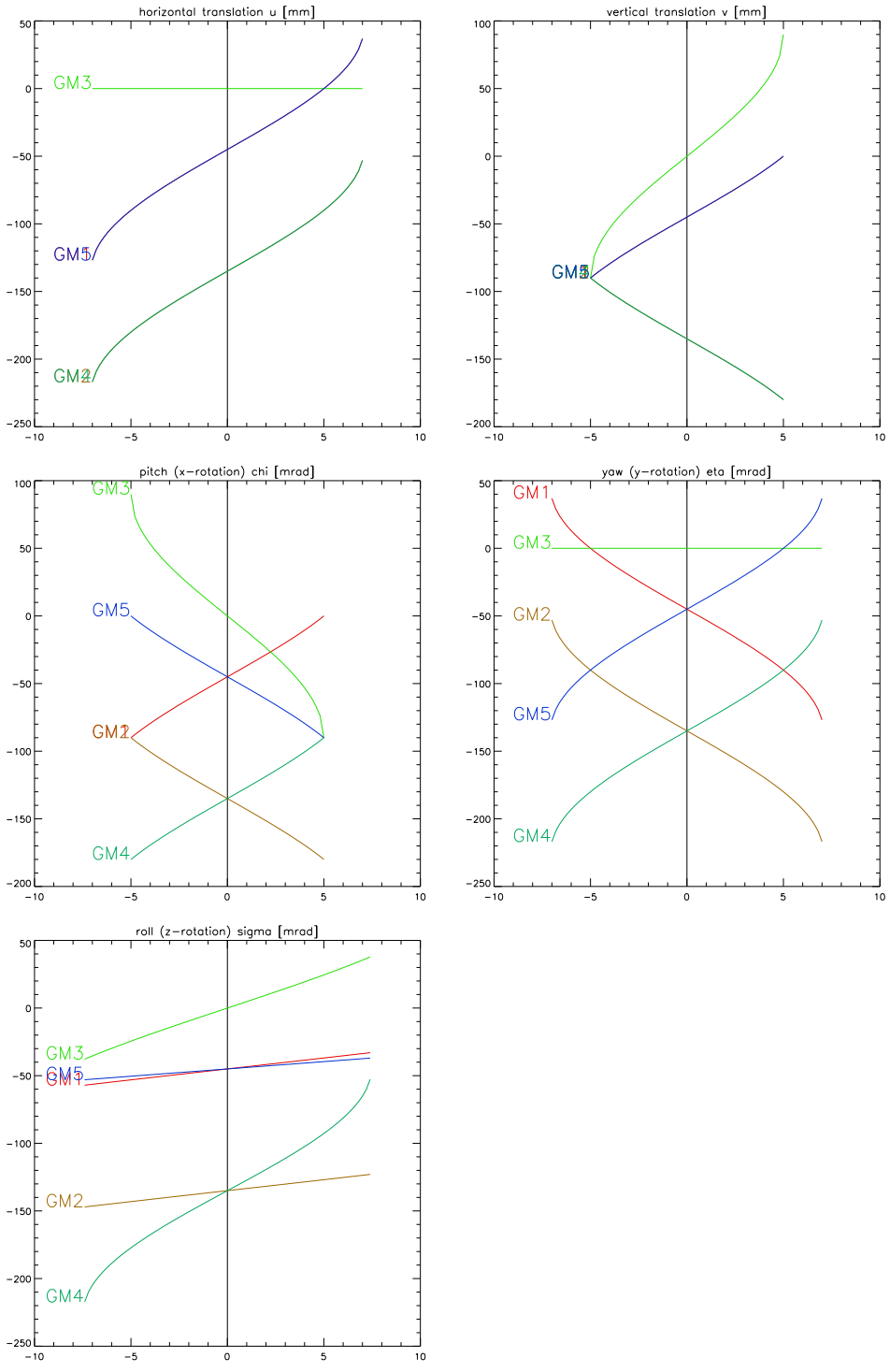

Figure 5: Excenter angles (linearized) as functions of single girder misalignments for the short girder

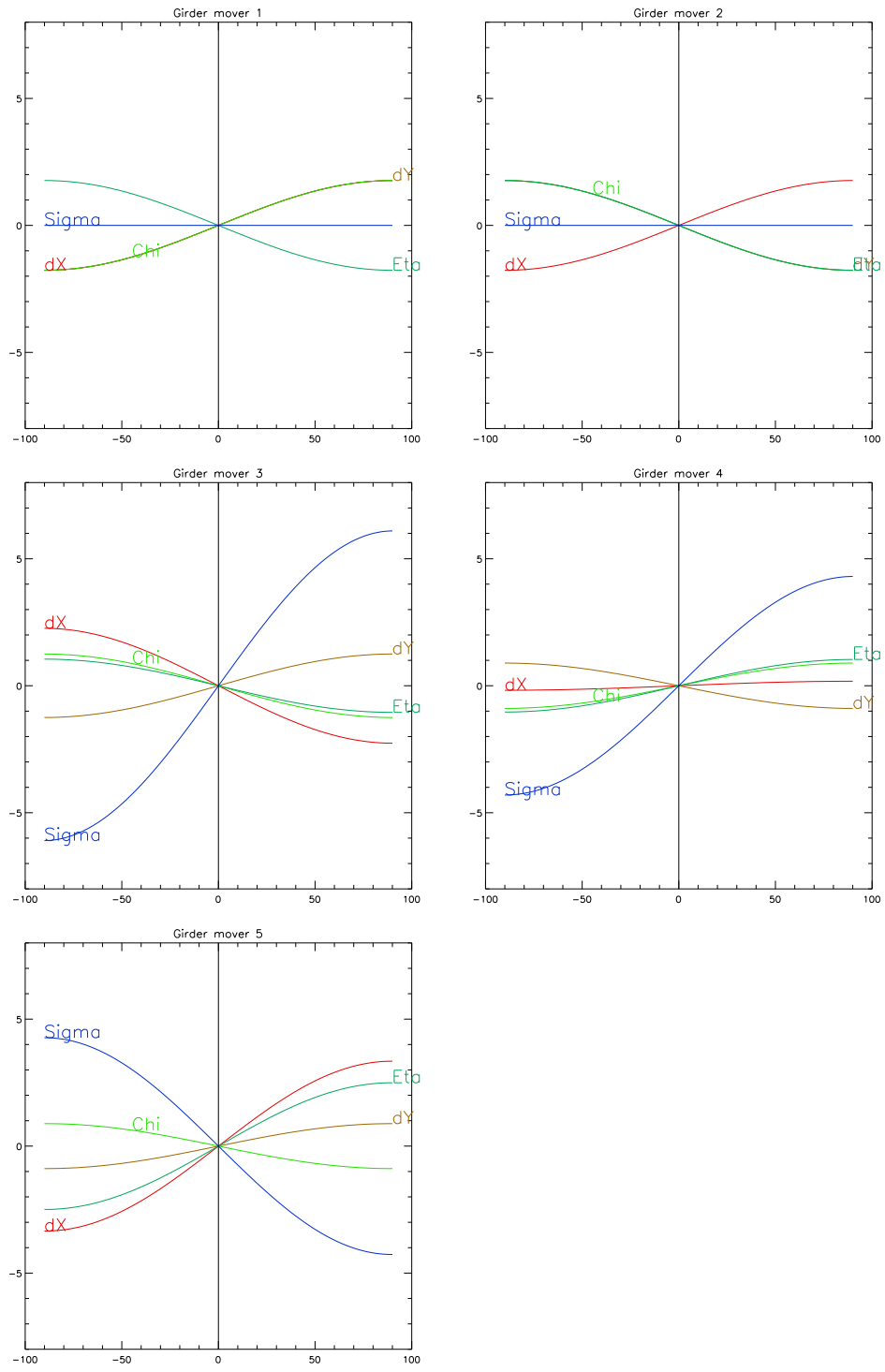

Figure 6: Misalignments as functions of single excenter excursion while keeping the other excenters at ideal positions

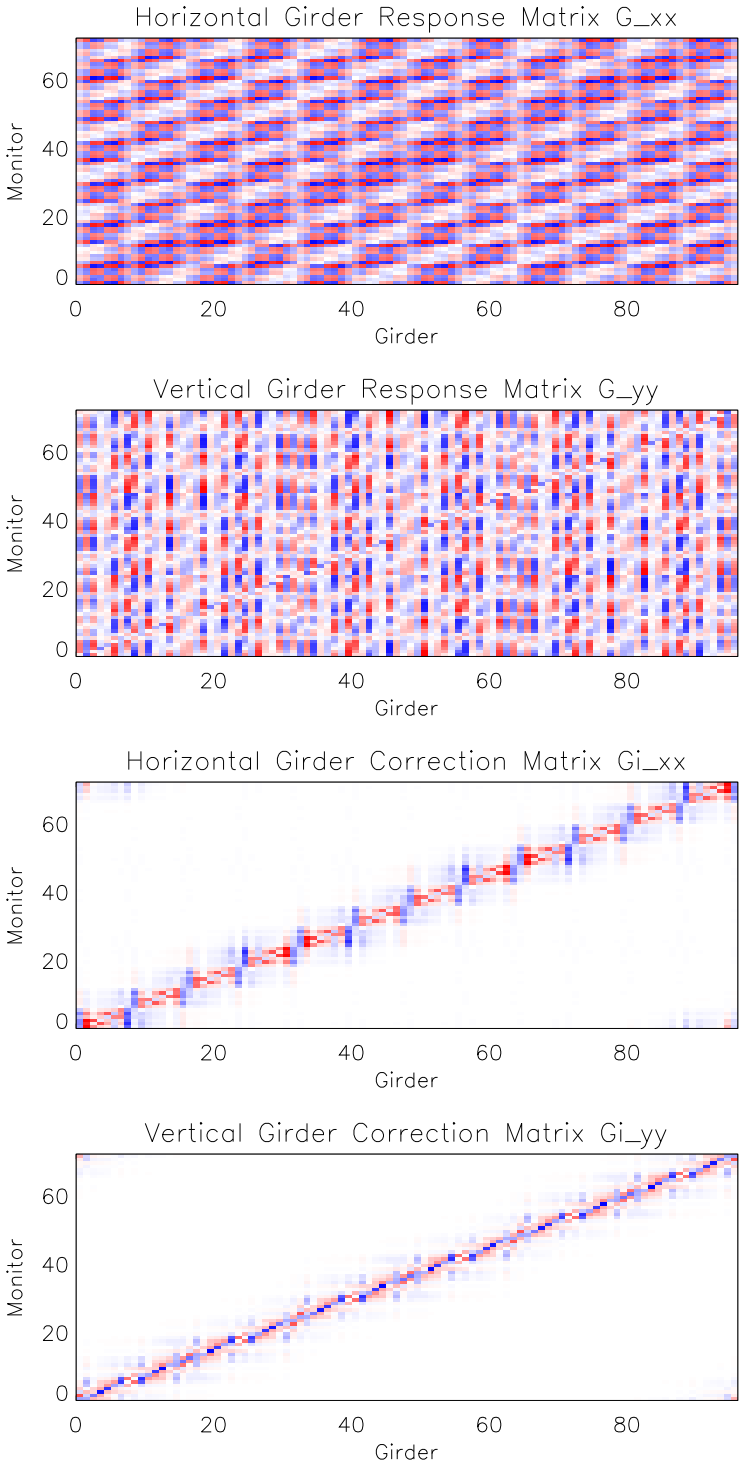

Figure 7: Girder response and correction matrices

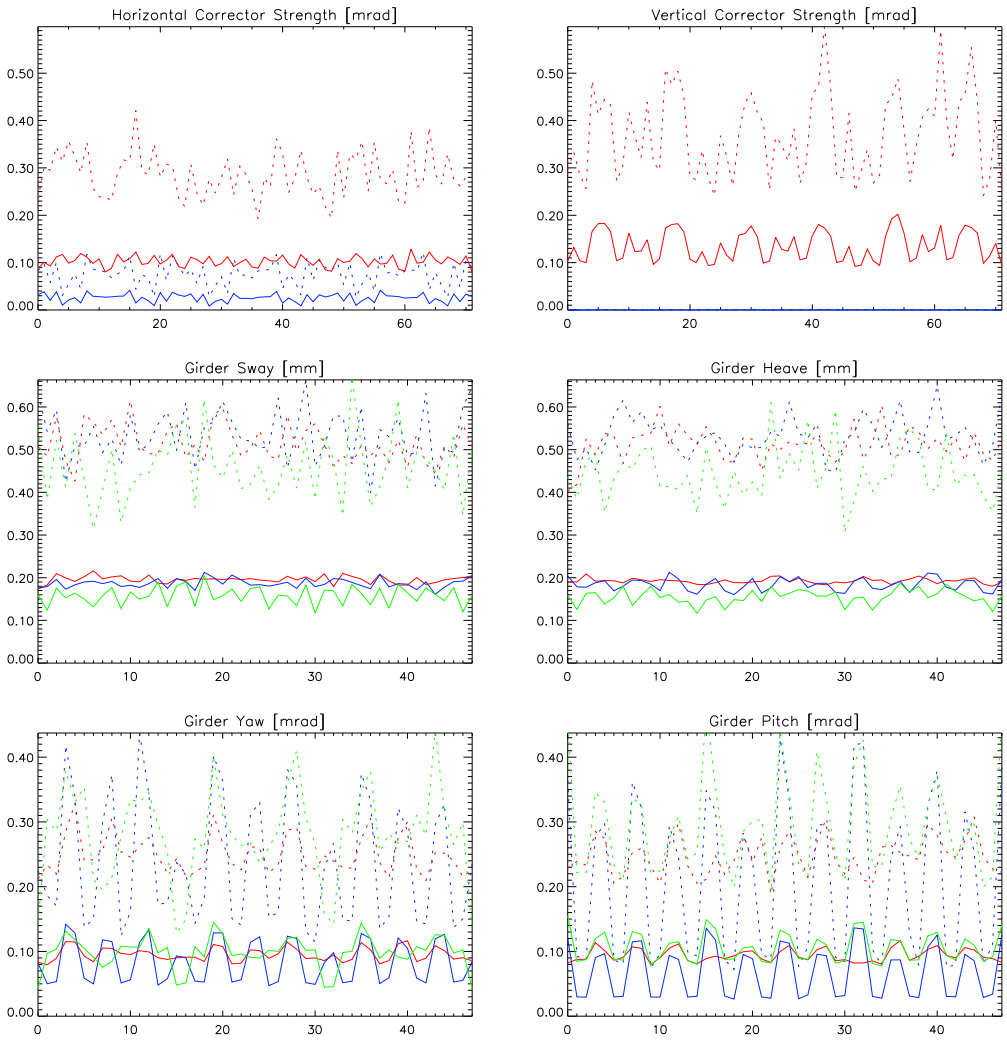

Figure 8: Beam based girder alignment: Corrector strengthes and girder misalignments for doing closed orbit corrections without (red) and with (blue) preceding beam base alignment of the girders. Maxima (dashed) and rms (solid) values from a 188 valid of total 200 random seeds are given. The green curves give the change in girder parameters. The application of random errors assumed partial train links over four girders (one sector) with an rms (cut at 2 sigma) displacement error of 300 μm for the [virtual] girder joints, 100 μm for the joint play (i.e. the precision of HLS and HPS systems) and 50 μm for the mounting of magnets and BPMs relative to the girder. No roll errors were applied. The SVD weight factors were filtered by the constrain $\omega_i > 0.001 \cdot \omega_{\max}$ and and reduced the set of girder parameters free for closed orbit correction to 60 out of 96 in the horizontal, leading to a residual orbit after girder alignment and nonzero corrector strengthes (blue). In the vertical the system is less degenerate and all 96 parameters were free to center the beam in 72 BPMs. resulting in zero corrector strength, i.e. the [static] vertical closed orbit correction is covered completely by beam based girder alignment.

Table 3: Girder midpoints and orientations in the SLS coordinate system (in mm)

n	X	Y	Z	Φ	g
1	41533.573	1400.000	16465.118	348.0	1400.0
2	40207.879	1400.000	21088.361	340.0	1400.0
3	37762.434	1400.000	25887.817	326.0	1400.0
4	35069.027	1400.000	29380.543	318.0	1000.0
5	30505.556	1400.000	34448.790	318.0	1000.0
6	27313.502	1400.000	37492.532	310.0	1400.0
7	22795.956	1400.000	40426.260	296.0	1400.0
8	18717.035	1400.000	42104.345	288.0	1000.0
9	9605.913	1400.000	45064.728	288.0	1000.0
10	5319.643	1400.000	46104.659	280.0	1400.0
11	-59.531	1400.000	46386.569	266.0	1400.0
12	-4431.023	1400.000	45800.373	258.0	1000.0
13	-11101.990	1400.000	44382.415	258.0	1000.0
14	-15333.974	1400.000	43139.886	250.0	1400.0
15	-20133.430	1400.000	40694.441	236.0	1400.0
16	-23923.414	1400.000	37733.382	228.0	1400.0
17	-35025.997	1400.000	27736.570	228.0	1400.0
18	-38366.997	1400.000	24276.864	220.0	1400.0
19	-41300.725	1400.000	19759.319	206.0	1400.0
20	-42978.810	1400.000	15680.397	198.0	1000.0
21	-45086.306	1400.000	9194.191	198.0	1000.0
22	-46126.237	1400.000	4907.921	190.0	1400.0
23	-46408.147	1400.000	-471.253	176.0	1400.0
24	-45821.951	1400.000	-4842.745	168.0	1000.0
25	-43830.157	1400.000	-14213.399	168.0	1000.0
26	-42587.628	1400.000	-18445.384	160.0	1400.0
27	-40142.183	1400.000	-23244.840	146.0	1400.0
28	-37448.776	1400.000	-26737.565	138.0	1000.0
29	-32885.305	1400.000	-31805.813	138.0	1000.0
30	-29693.251	1400.000	-34849.554	130.0	1400.0
31	-25175.706	1400.000	-37783.283	116.0	1400.0
32	-20716.361	1400.000	-39584.975	108.0	1400.0
33	-6507.577	1400.000	-44201.689	108.0	1400.0
34	-1840.883	1400.000	-45365.226	100.0	1400.0
35	3538.290	1400.000	-45647.136	86.0	1400.0
36	7909.782	1400.000	-45060.940	78.0	1000.0
37	14580.749	1400.000	-43642.982	78.0	1000.0
38	18812.734	1400.000	-42400.453	70.0	1400.0
39	23612.189	1400.000	-39955.008	56.0	1400.0
40	27104.915	1400.000	-37261.601	48.0	1000.0
41	34224.242	1400.000	-30851.330	48.0	1000.0
42	37267.984	1400.000	-27659.276	40.0	1400.0
43	40201.712	1400.000	-23141.730	26.0	1400.0
44	41879.797	1400.000	-19062.809	18.0	1000.0
45	43987.293	1400.000	-12576.603	18.0	1000.0
46	45027.224	1400.000	-8290.332	10.0	1400.0
47	45309.134	1400.000	-2911.159	-4.0	1400.0
48	44639.773	1400.000	1851.592	-12.0	1400.0